Received 21 May 2023, accepted 20 June 2023, date of publication 22 June 2023, date of current version 29 June 2023.
Digital Object Identifier 10.1109/ACCESS.2023.3288834

RESEARCH ARTICLE

2D Bipolar Optical Codes Based Concurrent Transmitting LiDAR With Code-Inversion Keying-Based Prime-Permuted Code

GUNZUNG KIM[1], (Member, IEEE), JEONGSOOK EOM[2], AND YONGWAN PARK[3], (Member, IEEE)
[1]Institute of Information and Communication, Yeungnam University, Gyeongsan, Gyeongsangbuk-do 38541, Republic of Korea
[2]Department of Information and Multimedia Engineering, Yeungnam University, Gyeongsan, Gyeongsangbuk-do 38541, Republic of Korea
[3]Department of Information and Communication Engineering, Yeungnam University, Gyeongsan, Gyeongsangbuk-do 38541, Republic of Korea
Corresponding author: Yongwan Park (ywpark@yu.ac.kr)

This work was supported by the Basic Science Research Program through the National Research Foundation of Korea(NRF) funded by the Ministry of Education under Grant NRF-2021R1A2B5B02086773, Grant NRF-2021R1A6A1A03039493, and Grant NRF-2022R1I1A1A01070998.

ABSTRACT We proposed a concurrent transmitting-based 128 channels LiDAR using an bipolar optical code scheme called code-inversion keying based prime-permuted code, which is the most suitable method to shorten the chip sequence length, while maintaining the performance characteristics of LiDAR. In each channel, four laser diodes with different wavelengths are bundled with a coupler to direct toward a target direction. The target direction could be recognized after the reception by identifying the received reflected pulse, even if several target directions were measured simultaneously. Due to the very short chip sequence, only a very short signal transmission time is required.

INDEX TERMS LiDAR, optical communication, bipolar optical codes, time-of-flight.

I. INTRODUCTION

Light detection and ranging (LiDAR) aims to obtain high-resolution 3D distance images with high refresh rates from long distances [1], [2]. All LiDARs use the time-of-flight (ToF) principle to estimate distance. The ToF is linearly proportional to the maximum distance of LiDAR. During ToF, the LiDAR actively listens to a transmission channel and waits for a reflected pulse to arrive. In a pulsed LiDAR, the ToF is idle listening time and the most time-consuming activity in distance estimation. The key performance indicators are the maximum distance, longitudinal resolution, distance precision and accuracy, lateral resolution, horizontal field-of-view, vertical field-of-view, and frame refresh rate [3], [4], [5], [6]. These key indicators are mutually related, and improving one can degrade the others [7]. For example, a low refresh rate (per second) is required for a high lateral resolution, as the maximum distance is proportional to the maximum pulse repetition rate. All the performance indicators of a pulsed LiDAR are directly related to idle listening time. The idle listening time particularly in pulsed LiDAR, is a significant obstacle in improving multiple performance indicators simultaneously.

The associate editor coordinating the review of this manuscript and approving it for publication was Rongbo Zhu.

Another problem is the range ambiguity [3], [8], for which a random pattern technique [9], [10] and multiple pulse repetition rates [11] were introduced. This method uses the correlation between the transmitted and received pulse patterns to identify the unique target ToF, but discriminating between low-intensity reflected pulses in the presence of high-intensity return pulses is challenging. Moreover, the listening time for reception increases with the maximum distance [12]. As an alternative to overcome the limitations of pulsed LiDAR, various LiDARs using modulated codes have been proposed. Optical communication transmits and receives a modulated laser signal using a high-quality optical cable without signal loss or attenuation. In order for LiDAR to measure the distance to an object, it needs to transmit a laser signal through the air and receive only the reflected signal when it hits the object. Unipolar communication sends and receives data using a pattern composed of the presence or absence of pulses, and the pulsed LiDAR measures the distance using the time when the transmitted pulse is reflected and received. Among the modulation codes used in optical communication, the unipolar code matches the characteristics of LiDAR very well. Both technologies have in common that they are based on the intensity of pulses, so they are very easy to converge. The unipolar method has a limit in improving the performance of LiDAR because it takes a very long time to transmit the laser pulse pattern according to the chip sequence. The bipolar code schemes use only a very short chip sequence, and the time to transmit the laser pulse pattern is short, so it is very suitable for improving the performance of LiDAR. LiDAR uses the reflected laser pulse to measure the distance, and among the bipolar communication methods in which the characteristics of the pulse change due to the influence of the reflected wave cannot be used. We reviewed the characteristics of various communication methods and selected the code inversion keying (CIK) based prime permuted code (CPPC) as the optimal bipolar method applicable to LiDAR.

LiDAR for vehicles is used in real space, and most LiDARs follow the regulations of accessible emission limit (AEL) Class 1. The maximum distance of LiDAR is inversely proportional to the intensity of the laser pulse. A pulsed LiDAR needs a large signal-to-noise ratio (SNR) to reduce false positives. However, pulse-coded LiDAR can reduce false positives even with a small SNR because it uses information from multiple pulses. The optical code scheme significantly influences the performance and characteristics of pulse-coded LiDAR [13]. As the number of laser pulses in the optical code increases, weaker laser pulses must be used to comply with AEL. In addition, the maximum distance is not significantly affected compared to the increased number of pulses and reduced pulse intensity.

Moreover, if the number of laser pulses increases, distances measured by multiple pulses can be used, reducing noise and improving the precision and accuracy of the measured distances. If the number of time bins for the optical code increases, the time to transmit the code to a target direction increases. Since LiDAR measures the distance only when the laser pulse is reflected and received, the longer the maximum distance measured, the longer the laser pulse flight and listening time for the reflected pulse, and the smaller the number of frame refresh rates. Most significantly, it uses a different signature for each distance target direction and measures another point without listening time, which requires the laser to be reflected and received from the target direction. As the transmission time increases, the number of frame refresh rates decreases because the dwell time of each measurement increases. Reducing the number of measurements by increasing the distance between target directions can increase the number of frame refresh rates. If the angle between the target directions widens, the minimum target object size increases, reducing the lateral resolution. Since the optical code determines the important performance indicators, the most important being the maximum distance, lateral resolution, and frame rates, optical code selection is the most challenging design factor. With long distances and high lateral resolution, LiDAR can provide improved 3D information for recognizing the surrounding environment. In the automotive sector, LiDAR is assumed as the next step towards full driverless capabilities as it can provide a high resolution and real-time 3D representation (point cloud) of the environment [1], [2].

This study proposed a concurrent transmitting LiDAR with bipolar optical codes with the following contributions to overcome the issues of maximum distance and high lateral resolution in LiDAR.

- A LiDAR with bipolar optical coded pulses that works with concurrent transmitting with body rotation is presented. The concurrent transmitting overcomes the limitation of low lateral resolution in traditional LiDARs, such as Velodyne LiDARs, and provides measuring for a further distance.
- The proposed 2D bipolar optical code scheme comprises bipolar optical code and dense wavelength division multiple access (DWDMA) to formulate the laser pulse wavelength. Our LiDAR can constantly measure long distances without idle listening time between target directions. The coded laser pulses include a unique identification number encoded by applying 2D bipolar optical code called CPPC. Therefore, this system transmits coded pulses in each target direction without the need for listening time for return pulses.
- Our LiDAR solves the range ambiguity problem and can discriminate between the previous and current pulses that overlap in the temporal domain.
- Extensive simulations were performed to evaluate the performance of the proposed LiDAR. Results indicate that our LiDAR performed better than conventional LiDARs in every aspect.

The remaining paper is organized as follows. Existing works on LiDAR with coded pulses are presented in Section II. Section III presents the architecture and working mechanism of the proposed LiDAR. Section IV describes the simulation setup, results, and analysis of the results. Finally, Section V presents the conclusion and future works.

II. SCANNING LIDAR WITH CODED PULSES

The transmitted laser power and received SNR mainly determine the maximum distance of the LiDAR. Both parameters are related to the received signal strength, but their approaches differ. It is possible to measure long distances by increasing the strength of the reflected received signal using a laser pulse with maximum power that does not exceed the AEL Class 1. Suppose the SNR is reduced to be close to one. Then, even a low-intensity reflected signal, similar to a long-distance noise, can be detected and used for distance measurement. In the case of radar and LiDAR, a large SNR is preferred because a low false alarm rate is essential, and high received signal strength is required. The maximum distance of the LiDAR refers to the furthest distance from which the received signal can be distinguished from noise. The received signal strength is inversely proportional to the square of the distance to the target. A strong reflected signal is received when the target is close, and vice versa. In the pulsed LiDAR, as the maximum power decreases, the maximum distance also decreases due to attenuation caused by the reflectivity and distance of target object. The received signal is clearly distinguished from noise when SNR is large; the false alarm rate is very low, but the maximum distance is shortened to increase the received signal strength. If SNR is low, the false alarm rate is high because the received signal is difficult to distinguish from noise. However, the maximum distance can increase as the received signal strength can be low.

In contrast, the coded pulse LiDAR has several potential differences from the conventional pulsed LiDAR. Replacing a single pulse with multiple pulses for a single target direction reduces the maximum power per pulse for AEL Class 1 compliance. The receiver utilizeutilizes multiple pulses reflected and received from one target direction in the optical code. Coded pulses are detected by signal correlation to measure long distances with high accuracy and precision, even with very low SNR. When multiple pulses are used for one target direction, the similarity in the pulse pattern in the transmitted and received pulses can be determined by analyzing their correlation. Even if the single laser pulse power is distributed and transmitted as multiple pulses, the reflected laser pulse can be detected with a low SNR, allowing object detection at a similar or longer distance compared to that of the single-pulse method.

Since the distance to the target is calculated by the time difference between the transmitted and received coded pulses, measuring the accurate ToF is necessary. A relatively large error in the pulse of the received signal can occur owing to the target's channel environment or physical reflection characteristics. A general LiDAR uses a Gaussian laser pulse; the received Gaussian laser pulse is broken due to the influence of noise in the reflection characteristic of objects and channel environment; this shape changes each time it is received. The original Gaussian shape cannot be restored precisely even after various approximation methods to the original Gaussian shape and the center of the damaged laser pulse by noise are applied. The standard for measuring the distance in the received laser pulse is based on the center point of the Gaussian laser pulse. The accuracy of the distance is also affected by the error generated by the shape of the laser pulse. Moreover, the received Gaussian pulse flights become distorted and deformed due to various noises, resulting in poor accuracy [14]. When using multiple laser pulses, even if individual laser pulses are affected by noise and there is a difference from the transmitted laser pulse type, the average of the multiple laser pulses can significantly reduce errors.

Unipolar coding schemes place one pulse in a chip sequence for a symbol and interpret the symbol using the pulse position. Cardinality, the number of simultaneously available users, is proportional to the chip sequence length. Prime number-based code schemes in optical communication use prime numbers larger than cardinality; the length of the chip sequence is proportional to the square of the prime number. The chip sequence becomes longer than the cardinality and the transmission time becomes longer. Code schemes using multiple laser wavelengths simultaneously address this problem by increasing the chip sequence proportionally to the prime number. The symbol is interpreted based on the position of the laser pulse at each laser wavelength. At least one laser pulse must be present in each wavelength in the code and should increase proportionally to the number of laser wavelengths. According to AEL regulations, multi-wavelength-based code schemes are disadvantaged because weak laser pulses shorten the maximum distance. However, the accuracy and precision increase proportionally with the number of laser pulses. In the unipolar method, the first laser pulse is placed on the first chip of the frame to recognize the pulse position in the frame. When the receiver detects the first laser pulse, it interprets it as a symbol according to the location of the laser pulse in the time bin. The laser pulse is in the first chip of all points simultaneously measured by LiDAR, and no laser pulses exist in the remaining chips because they are blank according to the code method. The chip's position with the laser pulse in the following chip sequence depends on the optical code scheme and symbols.

A. SEQUENTIAL TRANSMITTING LIDAR USING 1D UNIPOLAR OPTICAL CODED PULSES

The proposed LiDAR is based on unipolar direct-sequence optical code division multiple access (DS-OCDMA) that embeds the target direction information in its laser pulses [7]. Each channel is distinguished by a specific 1D unipolar optical code rather than a wavelength or time slot. An encoding procedure optically transforms each bit stream to a chip sequence before transmission. The reverse is performed at the receiver to decode the received signal stream and recover the original bit stream. The idle listening time is removed because the added laser pulses carry the target direction information, encoded using DS-OCDMA. The pulses are transmitted in each target direction without the listening time delay required to receive the reflected laser pulses in the conventional LiDAR. The sequential transmitting LiDAR uses a 905 nm laser pulse wavelength with a 5 ns pulse width and a MEMS mirror that scanned 10 times per second at a 128 × 128 resolution [15]. Fig. 1 shows the architecture of the sequential transmitting LiDAR, and Fig. 2 offers the operating strategy.

It is necessary to select an appropriate coding method for the LiDAR [13]. The asynchronous prime sequence code is an optical encoding scheme using a prime number larger than the number of concurrencies called cardinality. Each bit is encoded as a chip sequence. The code of the sequential transmitting LiDAR uses the presence or absence of laser pulses. However, not all chips have pulses, but there is one pulse

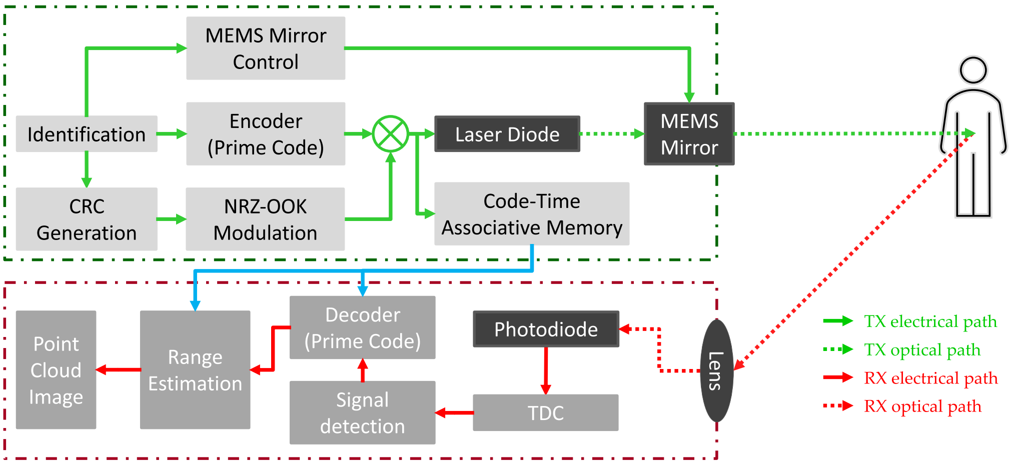

FIGURE 1. Architecture of the sequential transmitting LiDAR. The solid and dotted lines represent the electrical and optical signal paths, respectively. The green and red describe the transmission and reception operations, respectively.

for each prime number. The number of pulses for encoding one bit is the same as the prime number. The cardinality representing the maximum number of concurrency is a prime number, and the length of the chip sequence required is proportional to the squared prime number. Therefore, a prime number equal to or greater than the cardinality must be used for high cardinality. Since the chip sequence length required when encoding one bit is a squared prime number, one bit is converted into a row of chip sequences of long length. As the chip stream increases, the time required for transmitting increases proportionally to the product of the number of bits and the squared prime number.

As the transmitter encodes the bit stream to laser pulses using the asynchronous prime sequence code, the receiver separates and recognizes different laser lengths represented by several reflected waves that are received simultaneously [16], [17], [18], [19], [20], [21]. More than 9 different codewords are required to identify these laser pulses. Therefore, the one-dimensional unipolar asynchronous prime sequence code in the sequential transmitting LiDAR establishes a Galois field with prime number 11, $GF(11)$, that is 121 elements in length, 11 in weight, and represents 11 different codewords. When the spread spectrum on a 9-bit stream is implemented by multiplying each bit with a binary codeword of 121 chips, 1089 signals are generated. When a bit is "1," it is transformed into C_i, a binary codeword corresponding to 121 chips; when the bit is "0," the 121 chips are converted to "0." Each element ($s_{i,j}$) of the prime sequence ($S_i = (s_{i,0}, s_{i,1}, \ldots, s_{i,i}, \ldots, s_{i,10})$) based on the prime number 11 is determined using $s_{i,j} = ij(mod\ 11)$.

Each element ($c_{i,l}$) of the binary codeword ($C_i = (c_{i,0}, c_{i,1}, \ldots, c_{i,i}, \ldots, c_{i,120})$) that maps the prime sequence S_i is determined as follows.

$$c_{i,l} = \begin{cases} 1 & \text{if } l = s_{i,j} + 11j \text{ for } j = 0, 1, \ldots, 10 \\ 0 & \text{otherwise} \end{cases} \quad (1)$$

The sequential transmitting LiDAR sequentially measures the distance to a target using an encoded pulse. A LiDAR uses the elevation and azimuth angles of the spherical coordinate system to identify the target direction for measuring its distance. The azimuth and elevation angles are not separately distinguished in this sequential transmitting LiDAR. The target direction information represents the coded laser pulse based on the asynchronous prime sequence code. After generating and transmitting encoded laser pulses for one target direction, the MEMS mirror angle is adjusted to the next target direction without idle listening time for the reception of the reflected pulse. Then, a new encoding pulse is generated for the target direction, and the laser pulse is transmitted. The encoded bit stream with time is stored in the code-time associative memory and is used with the received time of the reflected pulse when calculating ToF. Thus, the encoded chip stream in the code-time associative memory is used for pulse detection, decoding, and ToF calculation in the receiver. The pulse is detected by the sliding window correlation method [22], [23] using the chip sequence stored in the code-time associated memory and generated as a pulse stream using the received signal. When the received laser pulse is decoded successfully, the target direction information can be known, and the transmitting time and distance are calculated.

The sequential transmitting LiDAR maintained the advantages of the maximum distance and improved measurement accuracy. Multiplexing via asynchronous prime sequence code allows measuring distances to multiple target directions simultaneously. Multiplexing support means sending multiple pulses to different target directions before the distance measurement of one target direction is finished, i.e., before receiving the reflected pulses from the current target direction. Even if reflected pulses from several target directions are received simultaneously, information about the target direction can be obtained by decoding the encoded content.

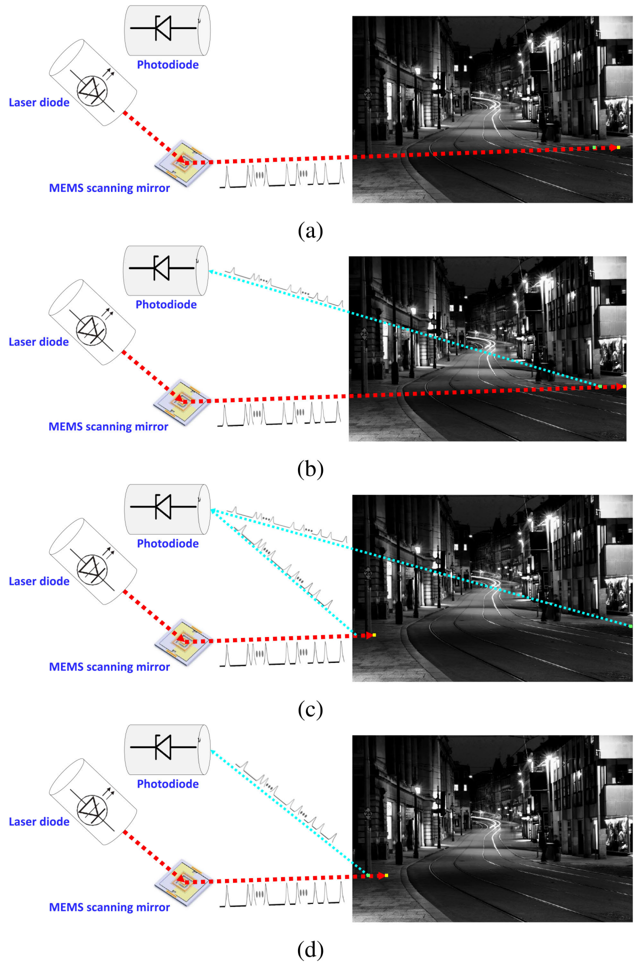

FIGURE 2. **Operating strategy of the sequential transmitting LiDAR with coded pulses. (a) LiDAR transmits coded pulse streams at the target, and the MEMS mirror is tilted towards the next target; (b) LiDAR repeats the (a) sequence. At the same time, the LiDAR receives a reflected pulse stream, decodes it, and then calculates the target distance with the identifier at the received pulse stream. (c) and (d) The LiDAR repeats the (b) sequence for all targets.**

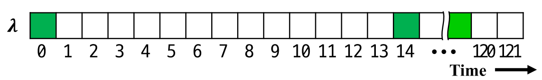

FIGURE 3. **LiDAR using asynchronous prime sequence code with one wavelength and 121 chips.**

In contrast, in the conventional simple pulse method, it is impossible to distinguish the target direction of the reflected pulse when several pulses are received simultaneously. Since it is possible to measure only one target direction at a time, the measurement time is constant based on the maximum distance. Hence, even if a laser pulse sent to the target direction is received, the distance to the next target direction is measured after a predetermined measurement time. In the sequential transmitting LiDAR, the incidence and reflection angles change according to the target direction, measured by reflecting the laser in the desired direction using a mirror. The laser pulse diameter reflected by the mirror is proportional to the cosine of the angle of incidence. The diameter increases when the incidence angle is close to a right angle. Hence, the received signal strength varied for the same distance.

B. CONCURRENT TRANSMITTING LIDAR USING 2D UNIPOLAR OPTICAL CODED PULSES

The concurrent transmitting LiDAR used several methods to overcome the limitation of the sequential transmitting LiDAR while using the advantages of the encoded pulse. A 2D OCDMA modulation was proposed in [24] and [25] that uses wavelength-hopping time-spreading codes for concurrent transmitting LiDAR. When transmitting laser pulses in the target direction, the concurrent transmitting LiDAR directly rotates the body with the attached laser sources. Fig. 4 shows the operation of the concurrent transmitting LiDAR [26], [27], [28], [29].

This concurrent transmitting LiDAR had a similar structure as Velodyne VLS-128, with 128 laser sources vertically attached to the LiDAR body. The LiDAR body is rotated to the target direction slightly and measured the distance to 360°. The pulse diameter is similar to the original pulse diameter when the angle of incidence is close to 0°. According to the measurement interval, this LiDAR had an azimuth angle of 360°, and 128 laser sources were mounted vertically to measure the elevation angle in each azimuth. The 128 elevation angles were divided by the wavelength of the laser source, and the azimuth angle used the encoded laser pulse based on 2D unipolar optical codes called the carrier-hopping prime code (CHPC). When the body rotates to measure the target distance, the same encoded laser pulses are generated from 128 laser sources using the azimuth information. Laser pulses of different wavelengths were transmitted according to the elevation angles. The wavelength has the elevation angle information of the received laser pulse needed to calculate the laser pulse transmitting time and distance to the target direction.

The proposed concurrent transmitting LiDAR has the following advantages over the sequential transmitting LiDAR. For sending laser pulses in the desired direction, the sequential transmitting LiDAR used the reflection of the MEMS mirror. However, the proposed LiDAR directly rotated the LiDAR body with laser sources attached to the body. Moreover, in the sequential transmitting LiDAR, the incidence and reflection angles changed according to the target direction, measured by reflecting the laser in the desired direction using a mirror. Thus, the received signal strength varied even at the same distance.

Fig. 5 shows the operating strategy of the concurrent transmitting LiDAR with coded pulses. Information for identifying the azimuth angle is encoded using a 2D unipolar optical codes. Each of the 128 sources generate encoded laser pulses using three laser diodes (LDs) with different wavelengths. The transmitter moves according to the desired azimuth as given by the azimuth information. The transmitting time is recorded while transmitting a laser at an elevation angle corresponding to each source using the multiplexer in

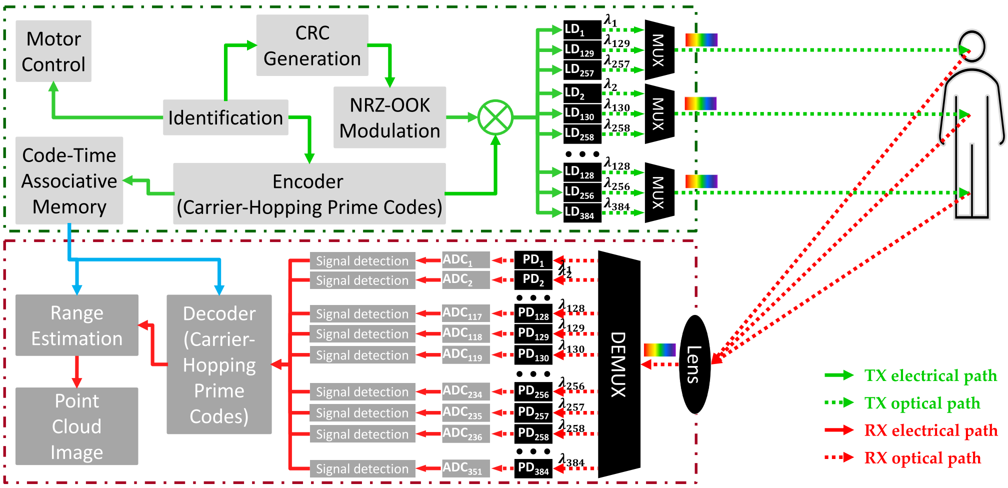

FIGURE 4. Architecture of the concurrent transmitting LiDAR based on 2D unipolar optical codes called carrier-hopping prime code (CHPC). The solid and dotted lines are the electrical and optical signal paths, while the green and red describe the transmission and reception operations, respectively.

each source. The encoded bit stream, stored with time in the code-time associative memory, is used for pulse detection, decoding, and ToF calculation in the receiver. The laser pulses fly toward the target direction at the speed of light and enter the receiver through the lens when reflected. The reflected waves are classified in the receiver according to the wavelength through the demultiplexer. Then it is converted into an analog electric signal using a photodiode to process the wavelength. After converting to digital data using ADC, the pulse is detected by the sliding window correlation method with chip sequence stored in the code-time associated memory and generated as a pulse stream using the received signal. The identification information was decoded using the 2D unipolar optical codes method, from which the time of transmitting the pulse was determined. The ToF and distance to the target are calculated and added to the point cloud image.

The wavelength used for the 2D unipolar optical codes method in the concurrent transmitting LiDAR was as follows. Vertically attached 128 laser sources required 384 wavelengths using three LDs to generate pulses of three different wavelengths. The 25 GHz signals have wavelengths from 1530.1389 nm to 1624.8914 nm, with the conventional band (C-band) defined for DWDM in ITU-T G.692 [18], [30]. In contrast, the 2D unipolar optical codes used by the concurrent transmitting LiDAR used several laser wavelengths. Fig. 6 expresses a 2D unipolar optical codes with three wavelengths, 11 chips, and 11 cardinality. This coding method can be identified according to the chip where the laser pulse is located at each wavelength.

Although multiple wavelengths reduce the transmitting time, the same number of laser pulses as the number of wavelengths is required. Reducing the power of every laser pulse to satisfy eye safety is difficult. Priority was given to the maximum distance in this LiDAR, so only three wavelengths were used. The asynchronous prime sequence code used one wavelength and required 121 chips of 11×11 for cardinality 11. 2D unipolar optical codes used three wavelengths, but only 11 chips for each wavelength to transmit the laser pulses. The transmitting time was reduced to a ratio of the square root of prime number. Then the pulse was transmitted in the target direction for a much shorter time. When using a pulse of 5 ns width, which is widely used in LiDARs, only 55 ns were required to transmit all the encoded laser pulses at the target direction. Therefore, using a narrow measurement angle allows quickly measuring 360°. 2D unipolar optical codes was generated using the following method. Given a set of k prime numbers $p_k \geq p_{k-1} \geq \ldots \geq p_1$, binary (0,1) matrices, $X_{i_k, i_{k-1}, \ldots, i_1}$, with ordered pairs [18], [25]:

$$
\begin{aligned}
&\{[(0,0), (1, i_1 + i_2 p_1 + \ldots + i_k p_1 p_2 \ldots p_{k-1}), (2, 2 \odot_{p1} i_1 \\
&\quad + (2 \odot_{p2} i_2) p_1 + \ldots + (2 \odot_{pk} i_k) p_1 p_2 \ldots p_{k-1}), \ldots, \\
&\quad \times (w-1, (w-1) \odot_{p1} i_1 + ((w-1) \odot_{p2} i_2) p_1 + \ldots \\
&\quad + ((w-1) \odot_{pk} i_k) p_1 p_2 \ldots p_{k-1})] : \\
&i_1 = \{0, 1, \ldots, p_1 - 1\}, i_2 = \{0, 1, \ldots, p_2 - 1\}, \ldots, \\
&i_k = \{0, 1, \ldots, p_k - 1\}\}
\end{aligned} \tag{2}
$$

for the 2D unipolar optical codes with cardinality $p_1 p_2 \ldots p_k$, $L = w$ wavelength, length $N = p_1 p_2 \ldots p_k$, and weight $w \leq p_1$, where "$\odot_{p_j}$" shows a module p_j n for $j = \{1, 2, \ldots, k\}$ [25].

III. CONCURRENT TRANSMITTING LIDAR USING 2D BIPOLAR OPTICAL CODED PULSES

We picked a 2D prime-permuted code, using Walsh codes for wavelength hopping and bipolar Barker sequences for time spreading, shortening the long chip sequence required in the unipolar optical codes of concurrent transmitting LiDAR and removing the start-of-frame bit [21]. Using incoherent on-off keying (OOK) modulation, every user sends a unipolar codeword corresponding to the address codeword of its intended

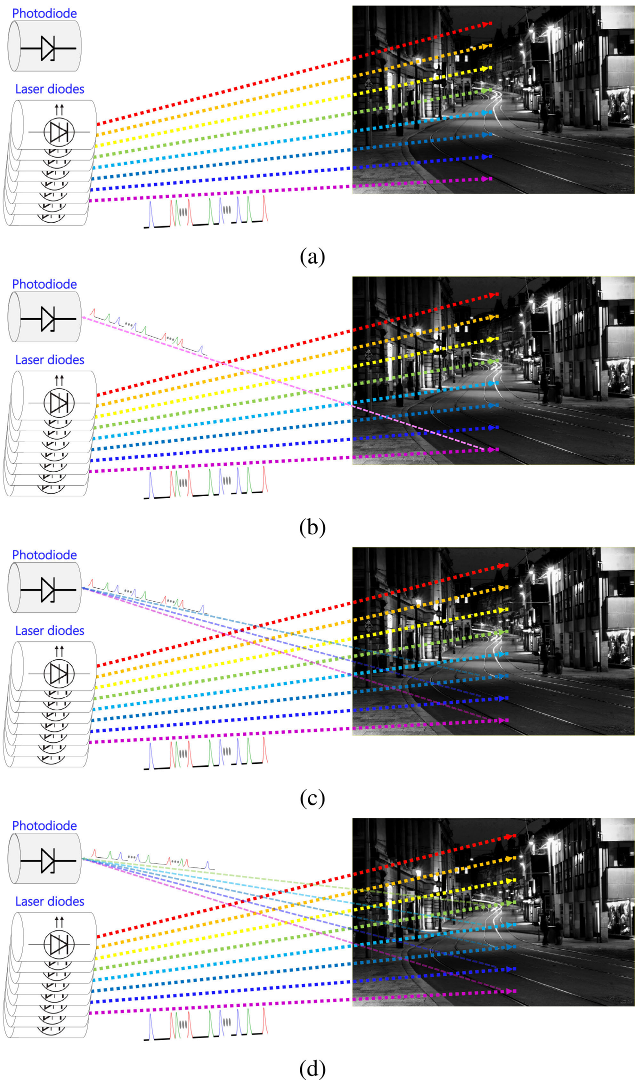

FIGURE 5. **Operating strategy of the concurrent transmitting LiDAR with 2D unipolar optical codes. (a) LiDAR transmits all coded pulse streams to each target all at once, and then, the body is rotated toward the next target detection; (b) LiDAR repeats (a). Simultaneously, the LiDAR receives a reflected pulse stream, decodes it, and calculates the target distance with the identifier at the received pulse stream. (c) and (d) LiDAR repeats (b) sequence for all targets.**

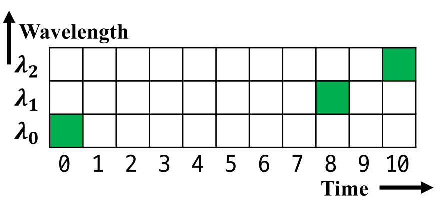

FIGURE 6. **LiDAR using carrier-hopping prime codes with three wavelengths and 11 chips.**

receiver for a data bit "1." However, nothing is transmitted for a data bit "0." Incoherent laser diodes are more cost-effective compared to coherent ones. Coherent laser diodes require complex and expensive components, such as high-quality optics and precise frequency stabilization techniques, which drive up the overall cost of the LiDAR [31].

TABLE 1. **Multiwavelength codewords and their wavelength conjugates based on the Walsh codes of length 4.**

Walsh code	Codeword	Wavelengths	Codeword	Wavelengths
$(+1-1+1-1)$	C_0	$\lambda_0\lambda_2$	$\overline{C_0}$	$\lambda_1\lambda_3$
$(+1+1-1-1)$	C_1	$\lambda_0\lambda_1$	$\overline{C_1}$	$\lambda_2\lambda_3$
$(+1-1-1+1)$	C_2	$\lambda_0\lambda_3$	$\overline{C_2}$	$\lambda_1\lambda_2$

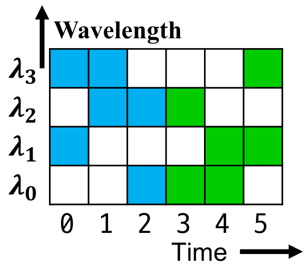

FIGURE 7. **LiDAR uses 2D bipolar optical codes called CIK-based $(4 \times 3, 3, 1, 1)$ prime permuted code over $GF(3)$ with three wavelengths and 6 chips. If codeword $C_0C_1\overline{C_2}$ is transmitted for a bit "1," the wavelength-conjugates, $\overline{C_0C_1}C_2$, are transmitted for a bit "0".**

Prime permuted codes support CIK, in which the "0" data bits are transmitted with wavelength-conjugate codewords and OOK. The permutations are controlled by the shifted prime sequences over $GF(p)$ of a prime p to keep the periodic cross-correlation functions of the 2D prime-permuted codes at most one [32], [33], [34], [35], [36], [37]. For the Walsh code of length four, four wavelengths represent the three multiwavelength codewords, as listed in Table 1. This table shows the wavelength mappings of the multiwavelength codewords, C_i, by the locations of the "+1" elements in the sequences. $\overline{C_i}$ denotes the wavelength-conjugate of C_i for $i = 0, 1, 2, 3$. In the CIK-based prime-permuted codes, the multiwavelength bipolar codes are permuted onto the time slots of the time-spreading bipolar codes of length N. The p^2 controls the permutation patterns shifted prime sequences over $GF(p)$ of a prime p, where $N \leq p$. Shown in Table 2 is the $(L \times N, \omega, 1, 1) = (4 \times 3, 3, 1, 1)$ prime-permuted code generated using the shifted prime sequences over $GF(3)$; L is the number of wavelengths, N is the length of Baker sequence [38] ω is the code weight; three multiwavelength codewords of length four, such as the Walsh code in Table 1; and the time-spreading Barker sequence $(+1, +1, -1)$ of length three. The "+1" and "−1" elements of the Barker sequence are represented by multiwavelength codewords, C_i's and $\overline{C_i}$'s, correspondingly, where the elements of the shifted prime sequences determine the index $i = 0, 1, 2, 3$. For CIK, the codes in Table 2 transmit the "1" data bits, while a wavelength-conjugate form transmits the "0" data bits. As shown in Table 1 and Fig. 7 if codeword $C_0C_1\overline{C_2}$ is transmitted for a bit "1," the wavelength-conjugates, $\overline{C_0C_1}C_2$, are transmitted for a bit "0."

Fig. 8 shows the operating strategy of concurrent transmitting LiDAR with 2D bipolar optical codes called CPPC.

TABLE 2. CIK-Based (4 × 3, 3, 1, 1) prime permuted code over *GF*(3) based on the multiwavelength codewords in Table 1 and time-spreading Baker sequence (+1 + 1 − 1).

Group $i=0$		Group $i=1$		Group $i=2$	
Codewords	Wavelengths	Codewords	Wavelengths	Codewords	Wavelengths
$C_0C_0\overline{C_0}$	$\lambda_0\lambda_2\lambda_0\lambda_2\lambda_1\lambda_3$	$C_0C_1\overline{C_2}$	$\lambda_0\lambda_2\lambda_0\lambda_1\lambda_1\lambda_2$	$C_0C_2\overline{C_1}$	$\lambda_0\lambda_2\lambda_0\lambda_3\lambda_2\lambda_3$
$C_1C_1\overline{C_1}$	$\lambda_0\lambda_1\lambda_0\lambda_1\lambda_2\lambda_3$	$C_1C_2\overline{C_0}$	$\lambda_0\lambda_1\lambda_0\lambda_3\lambda_1\lambda_3$	$C_1C_0\overline{C_2}$	$\lambda_0\lambda_1\lambda_0\lambda_2\lambda_1\lambda_2$
$C_2C_2\overline{C_2}$	$\lambda_0\lambda_3\lambda_0\lambda_3\lambda_1\lambda_2$	$C_2C_0\overline{C_1}$	$\lambda_0\lambda_3\lambda_0\lambda_2\lambda_2\lambda_3$	$C_2C_1\overline{C_0}$	$\lambda_0\lambda_3\lambda_0\lambda_1\lambda_0\lambda_2$

When measuring, laser pulses are sent out simultaneously from the 128 vertical channels, and distances are measured simultaneously. Each channel encodes and transmits identification information of target directions based on CPPC (4 × 3, 3, 1, 1). Four LDs with different wavelengths per channel are bundled with a coupler; hence, the lasers emitted fly toward the same target direction. When the laser transmission to the target direction is completed, it rotates to the next target direction without idle listening time for the reception of the reflected pulse. Since the cardinality of CPPC (4 × 3, 3, 1, 1) is nine, a unique non-overlapping code can be used for up to nine target directions. It takes 0.5 µs and 4.5 µs for one and nine target directions, respectively. Since the rotation angle between target directions is very narrow at 0.009°, one lens can sufficiently receive reflected waves up to 0.045°, the angle of the nine target directions. When converted to a measurable distance with ToF, it is 675 m theoretically, making it possible to measure a sufficiently long distance without mutual interference and listening time. The encoded chip stream is stored in the code-time associative memory with transmitting time and used with the received time of the reflected pulse when calculating ToF.

Fig. 9 shows the architecture of the concurrent transmitting LiDAR based on 2D bipolar optical codes. After generating a five-bit identification number according to the target direction, a three-bit CRC checksum is calculated to form an eight-bit transmission stream. The eight-bit transmission stream is encoded using CPPC (4 × 3, 3, 1, 1) to a chip sequence composed of 48 time-bins parallel to four wavelengths. The encoded chip stream stored in the code-time associative memory is used for pulse detection, decoding, and ToF calculation in the receiver. Four LDs with different wavelengths for each channel are bundled through a coupler in the transmitter. A total of 512 LDs with different wavelengths (between 1530.0413 nm and 1568.3623 nm for 12.5 GHz signal), and 128 wavelength intervals are spaced apart for each channel, allocated four each. If the time-bin value of the chip sequence of each wavelength is "1," the corresponding LD generates a laser pulse. It is sent to the target direction after combining it with other laser pulses through a coupler. When all pulse sequences are sent, the motor rotates to the next specified angle for the next target direction.

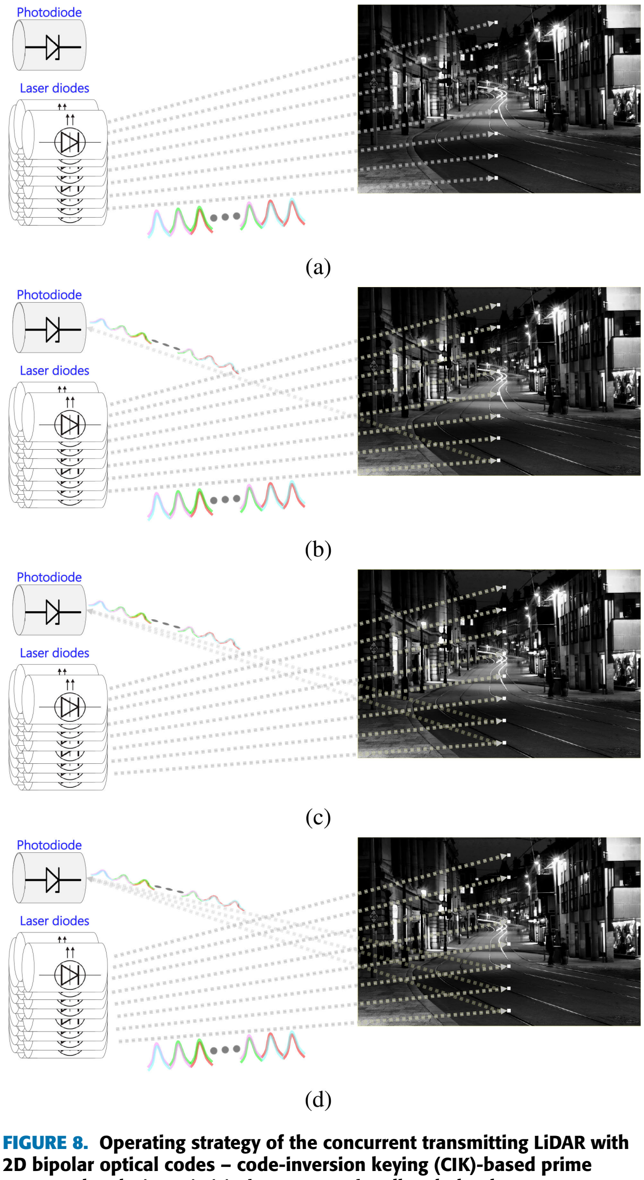

FIGURE 8. Operating strategy of the concurrent transmitting LiDAR with 2D bipolar optical codes – code-inversion keying (CIK)-based prime permuted code (CPPC). (a) LiDAR transmits all coded pulse streams to each target all at once and the body is rotated toward the next target detection; (b) LiDAR repeats (a). Simultaneously, the LiDAR receives a reflected pulse stream, decodes it, and then calculates the target distance with the identifier at the received pulse stream. (c) and (d) LiDAR repeats (b) the sequence for all targets.

After the emitted laser pulses are reflected from a target, they are received through the lens, divided into 512 wavelengths using a splitter, and transmitted to the ADC. The stream generated through the ADC limits the maximum signal value by applying the hard limit. The pulse is detected using the sliding window correlation method from the chip sequence stored in the code-time associated memory and generated as a pulse stream using the received signal. Four

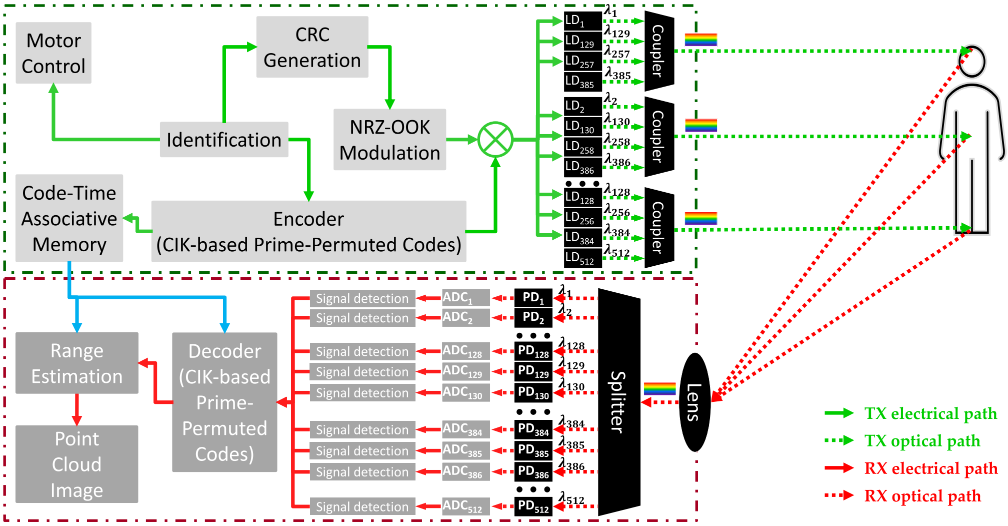

FIGURE 9. Architecture of the concurrent transmitting LiDAR based on 2D bipolar optical codes. The solid and dotted lines are the electrical and optical signal paths, while the green and red describe the transmission and reception operations, respectively.

pulse streams identical to the wavelength used for transmission are bundled. These are decoded using the CPPC (4 × 3, 3, 1, 1) stored in the code-time associative memory to generate a bit stream. A three-bit CRC is generated with five-bit identification information from the bit stream. The error is determined by comparing it with the three-bit CRC included in the bit stream. If there is no error, the distance to the object is calculated using the ToF method using channel and identification information and transmission and reception times. Finally, the point cloud is created by gathering the distance data information.

IV. SIMULATION

This section discusses the proposed concurrent transmitting LiDAR simulation results and compares its performance with other LiDARs. The environment in Fig. 10 was configured for the simulation to measure and compare the performance of the proposed LiDAR with that of other LiDARs. A white and black paper wall, 2 m wide and 2 m tall, was placed 2.5 m in front of the LiDAR. The reflectance of the white and black paper walls was 90 % and 10 %, respectively. For optical characteristics related to laser transmission/reception, reflection, and the lens, Synopsys RSoft OptSim optical simulation software was used [39]. In [7], the performance of the sequential transmitting LiDAR was evaluated by a prototype manufactured using a commercially available off-the-shelf product. We selected ADC12J4000 from Texas Instruments, a 12-bit, 4 GHz radio frequency-sampling ADC. The accuracy or drift depends mainly on the ADC. ADC12J4000 has 0.1 ps RMS as the ADC jitter or 0.03 mm in the distance. We chose parameters based on our previous prototype LiDAR for optical characteristics related to laser transmission and reception, pulse reflection, and lens. In [40], we described the components used in the simulation. MATLAB was used for encoding and decoding, signal processing, and distance calculation tasks.

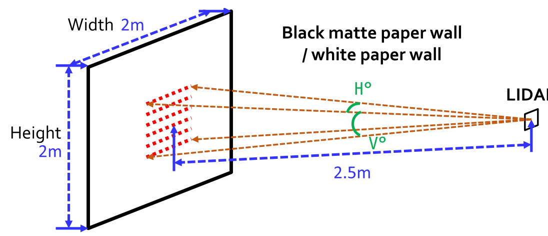

FIGURE 10. Environment used for simulating the four LiDARs.

A. SIMULATION ENVIRONMENT

We selected the VLS-128 LiDAR from Velodyne [41] and our previously developed 1D unipolar optical codes based sequential and 2D unipolar optical codes based concurrent transmitting LiDAR for performance comparison. The VLS-128 uses 128 infrared (IR) laser pairs with IR detectors for measuring the distance to the objects. The mounted body spins around its axis to scan a 360° environment, with each laser transmitted 18 500 times per second to produce a 3D point cloud. VLS-128 provides the highest resolution with the widest FoV in the world. The sequential transmitting LiDAR measured the target ten times per second with 128 azimuths and elevation angles each. The 2D unipolar optical codes based concurrent transmitting LiDAR measured the target 50 times per second with 20 000 azimuth and 128 elevation angles. A comparison is provided in Table 3. The width of the laser pulses used by the four LiDARs was 5 ns.

LiDAR snsors used in automobiles should comply with AEL Level 1. The wavelength and pulse width determines the laser output and the number of laser pulses used. The larger the number of laser pulses reaching the AEL standard

TABLE 3. Specification comparison of four LiDARs.

Item		Velodyne VLS-128	Sequential transmitting LiDAR based on 1D unipolar optical codes	Concurrent transmitting LiDAR based on 2D unipolar optical codes	Concurrent transmitting LiDAR based on 2D bipolar optical codes
Scene resolution		3600 × 128@5FPS	128×128@10FPS	20000 × 128@50FPS	40000 × 128@50FPS
Field-of-view (FoV)	Azimuth	360° (−180° to 180°)	40° (−20° to 20°)	360° (−180° to 180°)	360° (−180° to 180°)
	Elevation	40° (−20° to 15°)	40° (−25° to 15°)	40° (−25° to 15°)	40° (−25° to 15°)
Angular resolution	Lateral	0.1°	0.315°	0.018°	0.009°
	Elevation	0.315° (minimum)	0.315°	0.315°	ang0.315
Beam steering		Body rotation	MEMS mirror	Body rotation	Body rotation
Laser wavelength		903 nm	905 nm	1530.0413 nm to 1624.8914 nm (25 GHz spacing)	1530.0413 nm to 1624.8914 nm (12.5 GHz spacing)
Frame	Length	N/A	9 bit	9 bit	8 bit
	Structure	N/A	1 bit Start-of-Frame, 5 bit Identification, 3 bit CRC	1 bit Start-of-Frame, 5 bit Identification, 3 bit CRC	5 bit Identification, 3 bit CRC
Spreading method	Code scheme	N/A	Asynchronous prime sequence code	Carrier-hopping prime code	CIK-based prime permuted code
	Factor	N/A	Weight 11, length 121	Weight 3, length 11	Weight 3, length 4
	Cardinality	N/A	11	11	9
	Wavelength	N/A	1	3	4
	Line code	N/A	Unipolar NRZ	Unipolar NRZ	Bipolar
Pulse repetition frequency		200 MHz	200 MHz	200 MHz	200 MHz
Laser pulse energy		2.5 mJ	1.5 mJ	100.7 mJ	28.3 mJ
Laser pulse width		5 ns	5 ns	5 ns	5 ns
Chip sequence transmitting time		5 ns	5445 ns	495 ns	120 ns
Chip sequence transmitting method		8 transmits at once, 16 transmitting groups	One chip by one chip	One wavelengths at once, one chip by one chip	All wavelengths at once, one chip by one chip
Per target direction	Number of chips	N/A	1092	99 per wavelength, 297 per channel	24 per wavelength, 96 per channel
	Number of time bins	N/A	99	27	48
	Number of laser pulses	1	99	27	48
	Dwell Time	53.3 µs	6 µs	1 µs	0.5 µs
Per second	Number of targets	2 304 000	163 840	128 000 000	256 000 000
	Number of chips	N/A	178 421 760	12 672 000 000 per wavelength, 38 016 000 000 per channel	6 144 000 000 per wavelength, 24 576 000 000 per channel
	Number of laser pulses	2 304 000	16 220 160	3 456 000 000	12 288 000 000
AEL standard aperture	Time bins	5	10 890	14 850	9600
	Laser pulses	5	990	1350	4800

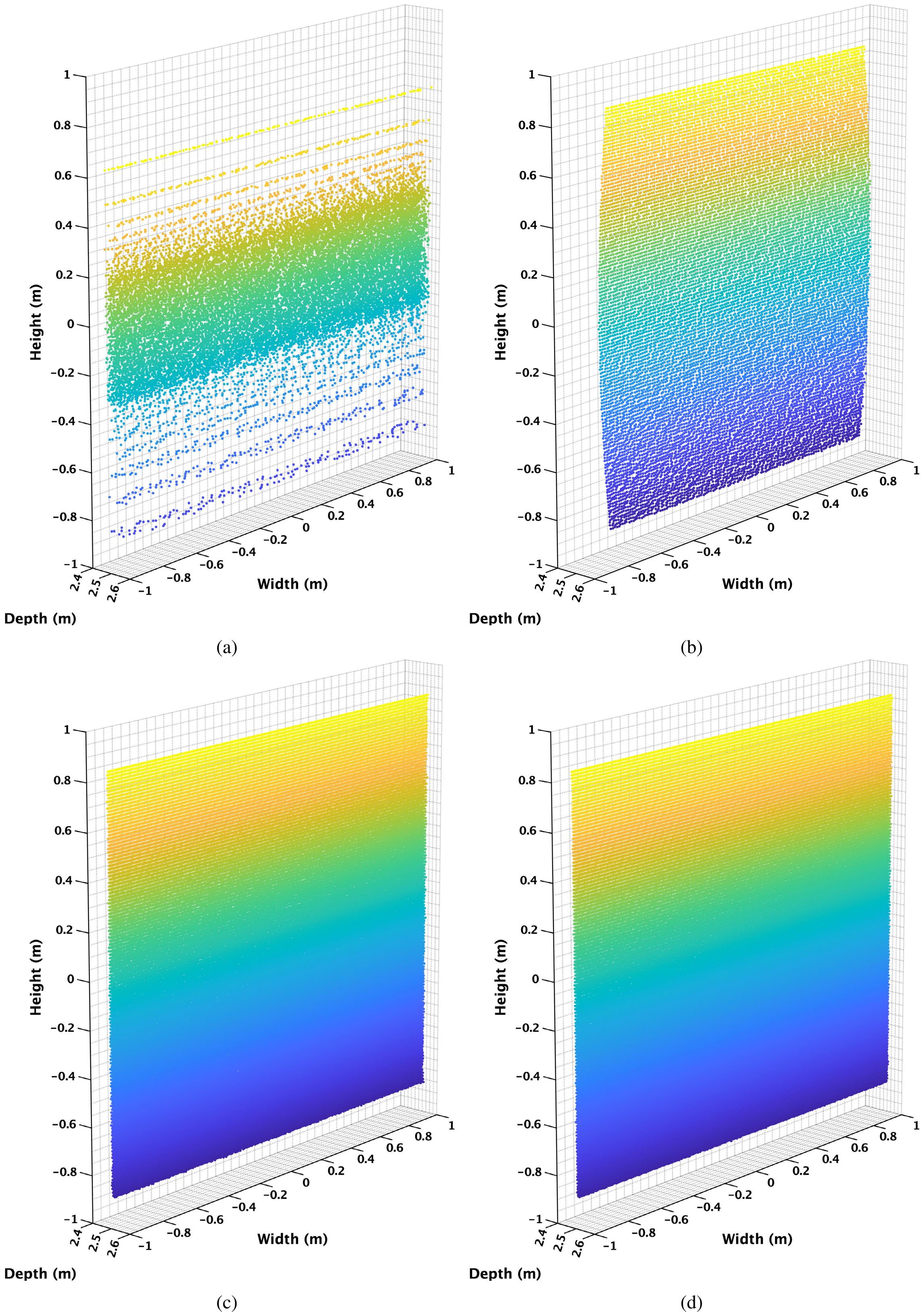

FIGURE 11. 3D point cloud generated by the four LiDARs. (a) Velodyne's VLS-128 scanning LiDAR. (b) Sequential transmitting LiDAR based on 1D unipolar optical codes. (c) Concurrent transmitting LiDAR based on 2D unipolar optical codes. (d) Concurrent transmitting LiDAR based on 2D bipolar optical codes.

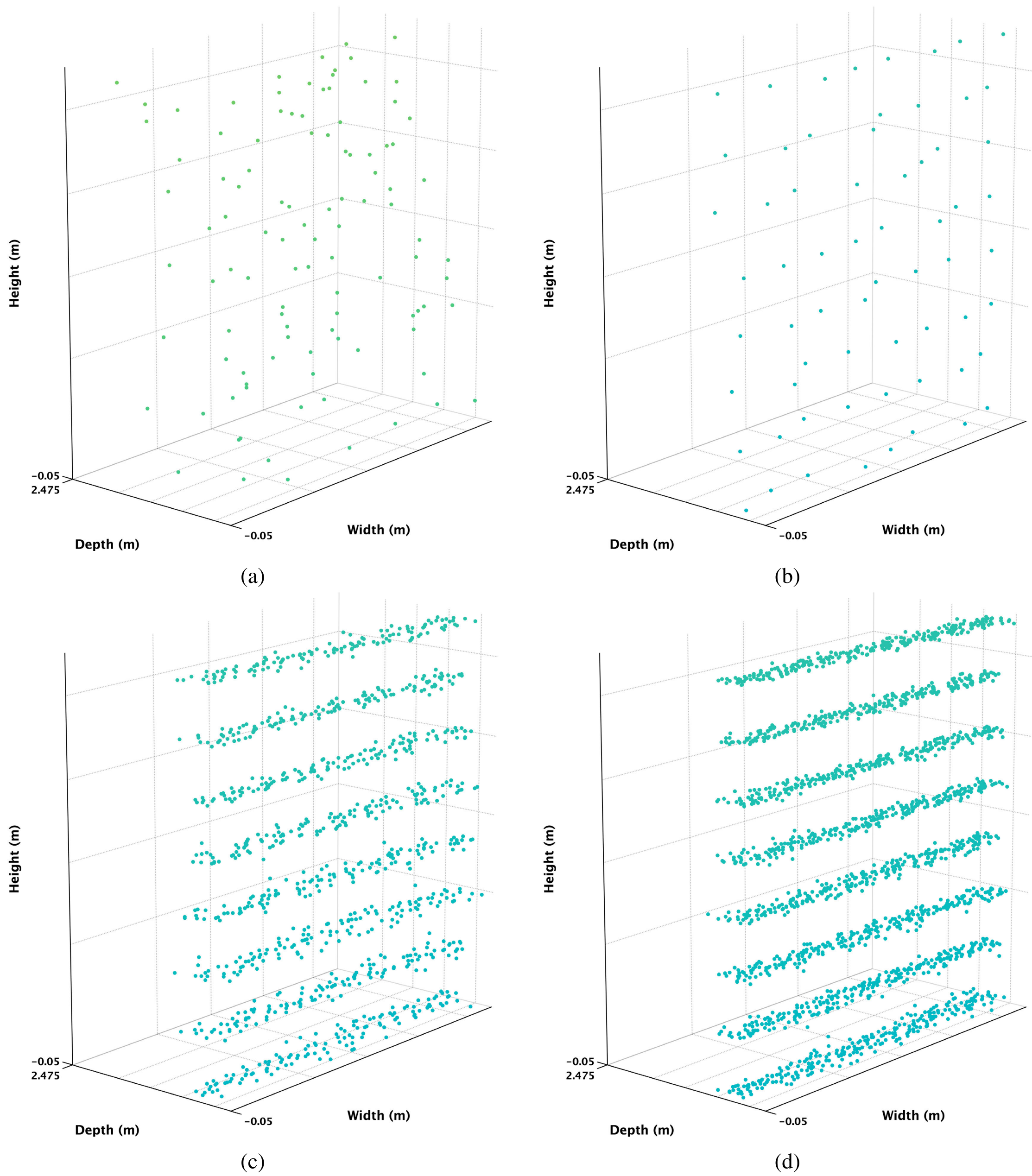

FIGURE 12. Center point zoomed 3D point cloud generated by the four LiDARs in Fig. 11. (a) Velodyne's VLS-128 scanning LiDAR. (b) Sequential transmitting LiDAR based on 1D unipolar optical codes. (c) Concurrent transmitting LiDAR based on 2D unipolar optical codes. (d) Concurrent transmitting LiDAR based on 2D bipolar optical codes.

aperture, the lower the power of the laser pulse. Of the three LiDAR snsors with coded pulses, the laser pulses transmitted from the sequential transmitting LiDAR arrived at the AEL standard aperture most frequently, and the concurrent transmitting LiDAR based on 2D unipolar optical codes arrived the least. By comparing the number of pulses, the 2D unipolar optical codes based concurrent transmitting LiDAR could use the highest laser power, and the sequential transmitting LiDAR used the lowest laser power to comply with AEL Class 1. The VLS-128 and sequential transmitting LiDAR use a laser in the near-infrared band near 900 nm, adversely affecting the human retina. However, the two concurrent transmitting LiDARs used a laser in the 1550 nm band, which is less harmful to the human retina. Hence, the highest laser power can be used even though the number of pulses of the 2D unipolar optical codes based concurrent transmitting LiDAR was the largest.

B. PERFORMANCE EVALUATION OF THE FOUR LIDARs

The properties of the LiDARs are summarized in Table 4 for further comparison. RSSI in Table 4 indicates the received signal strength indicator of the pulse. As shown in the

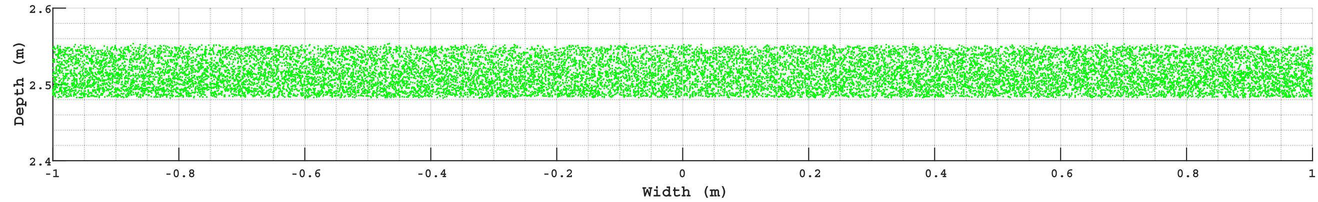

(a)

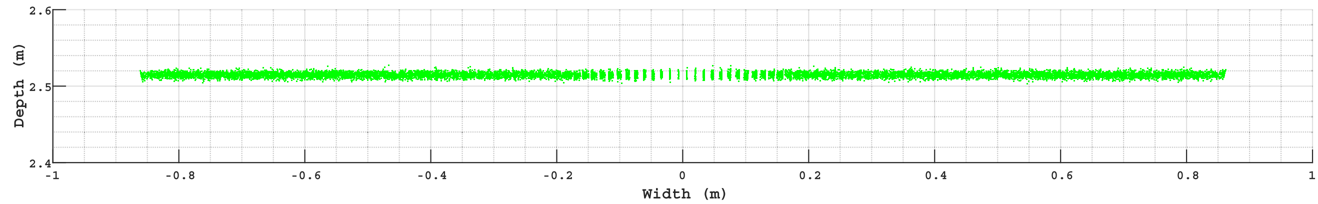

(b)

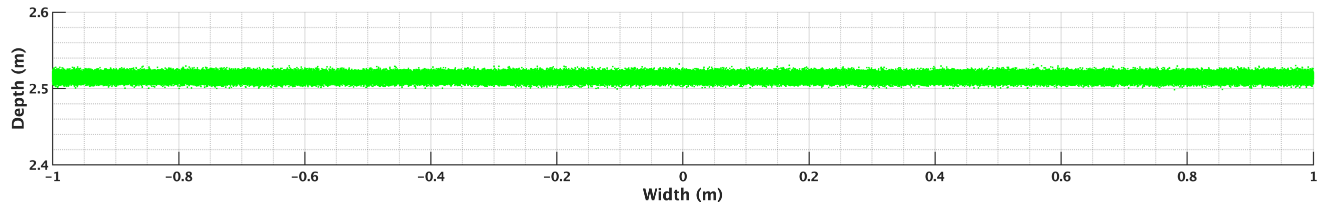

(c)

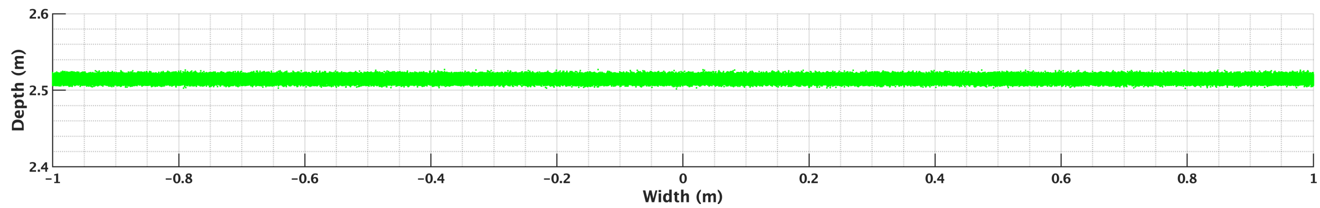

(d)

FIGURE 13. **Top view of the paper wall distances from the four LiDARs.**

TABLE 4. **Property comparison of the four LiDARs.**

Item		Velodyne VLS-128	Sequential Transmitting LiDAR based on 1D unipolar optical codes	Concurrent Transmitting LiDAR based on 2D unipolar optical codes	Concurrent Transmitting LiDAR based on 2D bipolar optical codes
Distance of two measured point	Azimuth	0.004 m	0.015 m	0.001 m	0.0005 m
	Elevation	0.005 m (minimum)	0.014 m	0.014 m	0.014 m
Number of measured point	Azimuth	458	128	2546	5093
	Elevation	127	116	116	116
Boundary of measured point	Up	0.669 m	0.67 m	0.67 m	0.67 m
	Left	−0.994 m	−0.909 m	−0.998 m	−0.999 m
	Right	0.994 m	0.909 m	0.998 m	0.999 m
	Down	−0.889 m	−0.994 m	−0.994 m	−0.994 m
Average RSSI of single pulse	Black paper	7134	92	10 937	1805
	White paper	64 158	912	98 094	16 483
Total RSSI of all pulses	Black paper	7134	4667	294 418	87 940
	White paper	64 158	42 031	2 650 064	791 896

measurement result, two concurrent transmitting LiDARs are the best, whereas the sequential transmitting LiDAR is the worst. The four LiDARs have the same FoV, but the number of measurements is different due to the difference in lateral resolution. VLS-128 has a non-linear distribution of lateral resolution in elevation, whereas the 2D bipolar optical codes based concurrent transmitting LiDAR had the best lateral resolution. Consequently, the number of locations where paper walls were measured was the largest for the 2D bipolar optical codes based concurrent transmitting LiDAR. The sequential

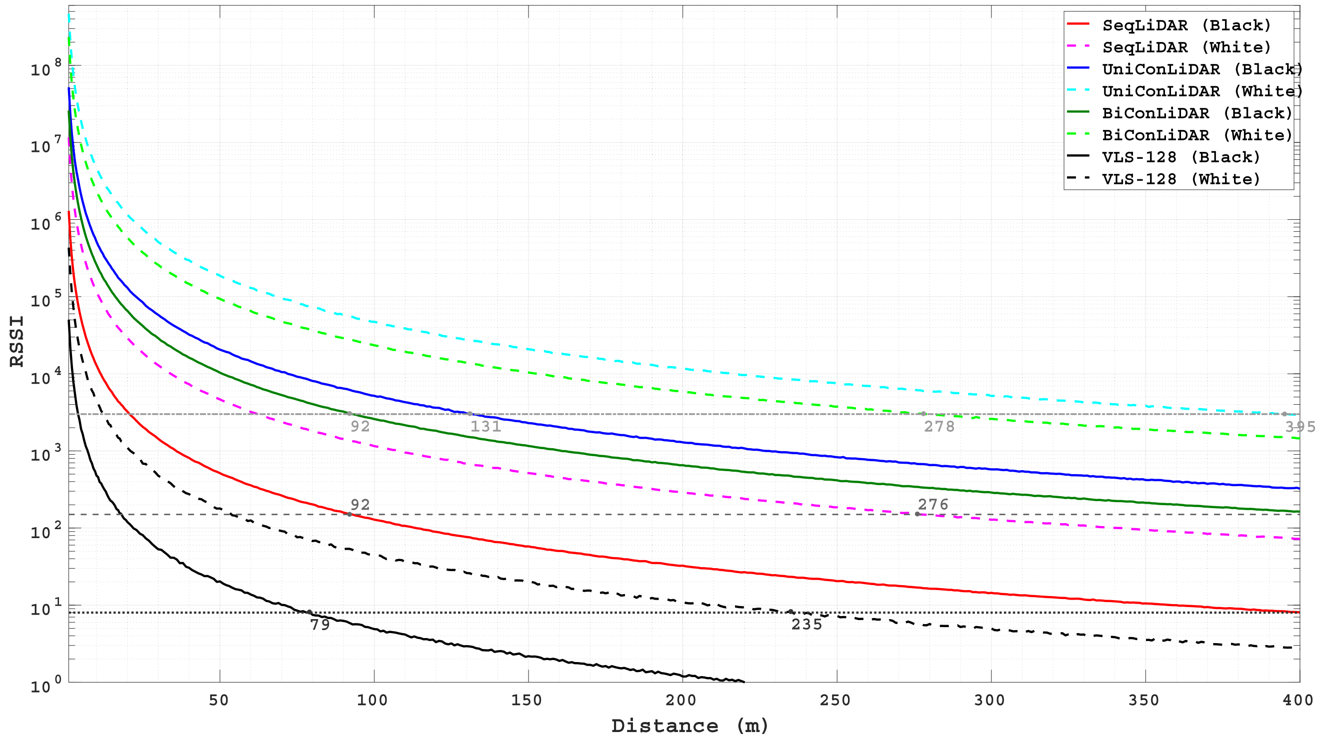

FIGURE 14. Received signal strength indicator and maximum distance of the four LiDARs. "SeqLiDAR" indicates the sequential transmitting LiDAR based on 1D unipolar optical codes [7]; "UniConLiDAR" is the concurrent transmitting LiDAR based on 2D unipolar optical codes [27]; "BiConLiDAR" is the proposed concurrent transmitting LiDAR based on 2D bipolar optical codes; "VLS-128" refers to the Velodyne VSL-128 LiDAR.

transmitting LiDAR has a poor lateral resolution, resulting in poor paper wall measurement.

Fig. 11 and 12 show the location data measured by the four LiDARs. The 3D point cloud generated by the proposed LiDAR was rich compared to the others. The sequential transmitting LiDAR has poor performance compared to VLS-128.

Fig. 13 shows the locations measured by the paper walls in the four types of LiDARs in a top-view format. These figures show the FoV and distance information of the azimuth angle for the measurement locations. The FoV is determined by the unique specifications of each LiDAR method, but the distance information represents a measuring error. According to the central limit theorem, the more data used in the calculation, the less the error and the better the accuracy and precision. The sequential transmitting LiDAR used the most laser pulses and has the least error, as shown in Fig. 13a. In contrast, the VLS-128, which uses only one laser pulse, has the largest error, as given in Fig. 13b. Although the proposed LiDAR used fewer laser pulses than the sequential transmitting LiDAR, there is no difference in the distance error. Thus, the proposed LiDAR exhibited precision and accuracy, similar to the sequential transmitting LiDAR, even with fewer laser pulses.

Fig. 14 shows the maximum detectable distance using the received signal strength when measuring the white and black matte paper walls with the three LiDARs. The sequential and concurrent transmitting LiDARs could detect signals that

TABLE 5. Maximum distance, accuracy, and precision of the four LiDARs.

Item	Velodyne VLS-128	Sequential transmitting LiDAR based on 1D unipolar optical codes	Concurrent transmitting LiDAR based on 2D unipolar optical codes	Concurrent transmitting LiDAR based on 2D bipolar optical codes
Maximum distance	238 m	278 m	394 m	280 m
Accuracy	0.047 m	0.029 m	0.029 m	0.029 m
Precision	0.019 m	0.002 m	0.003 m	0.002 m

were not clearly distinguished from noise using multiple reflected laser pulses. Compared to the black matte paper wall, the white paper wall had higher reflectivity, and the three LiDARs could equally measure a longer distance. The laser output of the sequentially transmitted LiDAR is lower than that of the VLS-128. However, reflected waves over a longer distance were detected using multiple reflected laser waves. The proposed LiDAR could transmit laser pulses with a power of several tens of times higher than that of sequential transmitting LiDAR or the VLS-128 using laser pulses in the 1550 nm band instead of the 900 nm band and fewer pulses for multiplexing. Thus, the measurable distance was longer than other LiDAR. Moreover, the received signal strength was inversely proportional to the square of the distance to the target direction. Strong and weak signals were received when the distance to the destination was near and far, respectively.

The position accuracy and precision were measured for the four LiDARs according to the American Society for Photogrammetry and Remote Sensing (ASPRS) standards [42], [43]. The simulation results are summarized in Table 5. The sequential transmitting LiDAR using multiple pulses performed slightly better than concurrent transmitting LiDARs and much better than Velodyne's VLS-128 LiDAR. Compared to the VLS-128, which uses one pulse, the sequential transmitting LiDAR had twice the accuracy, whereas the two concurrent transmitting LiDARs had five to six times higher accuracy.

V. CONCLUSION

This paper proposed a 2D bipolar optical codes based concurrent transmitting LiDAR that compensates for the shortcomings of the pulse-coded LiDAR. This system is a bipolar communication method that is not affected by reflected waves, and effectively overcomes the long transmission time of the unipolar communication method while maintaining good measurement characteristics of code-based LiDAR. The sequential transmitting LiDAR implements multiplexing using an asynchronous prime sequence code and requires a long chip sequence and the transmission of laser pulses to each target direction. The 2D unipolar optical codes based concurrent transmitting LiDAR uses a multiplexer to mix different wavelengths. The 2D bipolar optical codes based concurrent transmitting LiDAR uses an optical coupler to bundle multiple wavelengths. In the two concurrent transmitting LiDARs, 128 elevation angles can be measured simultaneously by transmitting laser pulses of different wavelengths from one azimuth angle. The 2D bipolar optical codes based concurrent transmitting LiDAR can operate much faster than other pulse-coded LiDARs and Velodyne's VLS-128. The sequential transmitting LiDAR and VLS-128 use the 900 nm band, which poses a severe threat to the human retina. The two concurrent transmitting LiDARs use the 1550 nm band, which only slightly influences the human optic nerve.

Extensive simulations were performed to analyze the characteristics and performance of the four LiDARs. Performance was analyzed for the 3D point cloud, maximum distance, precision, and accuracy. Results suggested that the 2D bipolar optical codes based concurrent transmitting LiDAR performed slightly better than the 2D unipolar optical codes based concurrent transmitting LiDAR and much better than the sequential transmitting and VLS-128 LiDARs. The proposed LiDAR uses 512 LDs and photodiodes, each in the 1550 nm band. These LDs are expensive and become the most significant factor contributing to the high price when commercialized. Depending on the product's target, coded pulses with larger LDs and photodiodes can increase the resolution as desired. Selecting an optical coding technique according to the LiDAR target is helpful. Using a 2D optical coding scheme such as that used for a concurrent transmitting LiDAR to increase the number of target directions and refresh ratio per second can maximize the distance measured even if accuracy and precision are compromised. The 1D optical coding scheme, such as that used for a sequential transmitting LiDAR, is preferable if accuracy and precision are prioritized. It is necessary to study the coded laser pulses so that they can be used when there are many LiDARs in a dense space in the future. Furthermore, side effects from using coded pulse streams need investigation. Due to the significant differences between the simulations and actual environment, the signal reflected by irregular objects can destroy the encoded pulse stream in reality. Hence, LiDARs cannot decode the received encoded pulse stream correctly.

REFERENCES

[1] D. Puschini, C. Karaoguz, O. El-Hamzaoui, and T. Rakotovao, "Are LIDARs ready for perception in future intelligent transportation?" in *Electronic Components and Systems for Automotive Applications Proceedings of the 5th CESA Automotive Electronics Congress, Paris, 2018*. Springer, 2019, pp. 161–171.

[2] R. Roriz, J. Cabral, and T. Gomes, "Automotive LiDAR technology: A survey," *IEEE Trans. Intell. Transp. Syst.*, vol. 23, no. 7, pp. 6282–6297, Jul. 2022.

[3] P. F. McManamon, *Field Guide to LiDAR*, Bellingham, WA, USA: International Society for Optics and Photonics, 2015.

[4] *LMS5xx 2D LiDAR Sensors*, SICK AG, Waldkirch, Germany, 2015.

[5] Z. Dai, A. Wolf, P.-P. Ley, T. Gluck, M. C. Sundermeier, and R. Lachmayer, "Requirements for automotive LiDAR systems," *Sensors*, vol. 22, no. 19, p. 7532, Oct. 2022.

[6] S. Royo and M. Ballesta-Garcia, "An overview of LiDAR imaging systems for autonomous vehicles," *Appl. Sci.*, vol. 9, no. 19, p. 4093, Sep. 2019.

[7] G. Kim and Y. Park, "LiDAR pulse coding for high resolution range imaging at improved refresh rate," *Opt. Exp.*, vol. 24, no. 21, pp. 23810–23828, Oct. 2016.

[8] P. F. Mcmanamon, "Review of Ladar: A historic, yet emerging, sensor technology with rich phenomenology," *Opt. Eng.*, vol. 51, no. 6, Jun. 2012, Art. no. 060901.

[9] P. A. Hiskett, C. S. Parry, A. McCarthy, and G. S. Buller, "A photon-counting time-of-flight ranging technique developed for the avoidance of range ambiguity at gigahertz clock rates," *Opt. Exp.*, vol. 16, no. 18, pp. 13685–13698, 2008.

[10] N. J. Krichel, A. McCarthy, and G. S. Buller, "Resolving range ambiguity in a photon counting depth imager operating at kilometer distances," *Opt. Exp.*, vol. 18, no. 9, pp. 9192–9206, Apr. 2010.

[11] Y. Liang, J. Huang, M. Ren, B. Feng, X. Chen, E. Wu, G. Wu, and H. Zeng, "1550-nm time-of-flight ranging system employing laser with multiple repetition rates for reducing the range ambiguity," *Opt. Exp.*, vol. 22, no. 4, pp. 4662–4670, 2014.

[12] R. D. Richmond and S. C. Cain, *Direct–Detection LADAR Systems* (Tutorial Texts in Optical Engineering), vol. 85. Bellingham, WA, USA: International Society for Optics and Photonics, 2010.

[13] G. Kim and Y. Park, "Suitable combination of direct intensity modulation and spreading sequence for LiDAR with pulse coding," *Sensors*, vol. 18, no. 12, p. 4201, Nov. 2018.

[14] Z. Gu, J. Lai, C. Wang, W. Yan, Y. Ji, and Z. Li, "Generalized Gaussian decomposition for full waveform LiDAR processing," *Meas. Sci. Technol.*, vol. 33, no. 6, Jun. 2022, Art. no. 065201.

[15] *Mirrocle Technologies MEMS Mirrors—Technical Overview*, Mirrorcle Technol., Richmond, CA, USA, 2016.

[16] F. R. K. Chung, J. A. Salehi, and V. K. Wei, "Optical orthogonal codes: Design, analysis and applications," *IEEE Trans. Inf. Theory*, vol. 35, no. 3, pp. 595–604, May 1989.

[17] A. S. Holmes and R. R. A. Syms, "All-optical CDMA using 'quasi-prime' codes," *J. Lightw. Technol.*, vol. 10, no. 2, pp. 279–286, Feb. 1992.

[18] G.-C. Yang and W. C. Kwong, *Prime Codes With Applications to CDMA Optical and Wireless Networks*. Norwood, MA, USA: Artech House, 2002.

[19] C. Goursaud-Brugeaud, A. Julien-Vergonjanne, and J.-P. Cances, "Prime code efficiency in DS-OCDMA systems using parallel interference cancellation," *J. Commun.*, vol. 2, no. 3, pp. 51–57, May 2007.

[20] A. M. Weiner, Z. Jiang, and D. E. Leaird, "Spectrally phase-coded O-CDMA," *J. Opt. Netw.*, vol. 6, no. 6, pp. 728–755, 2007.
[21] W. C. Kwong and G.-C. Yang, *Optical Coding Theory With Prime*. Boca Raton, FL, USA: CRC Press, 2013.
[22] R. T. Edwards, G. Cauwenberghs, and F. J. Pineda, "Optimizing correlation algorithms for hardware-based transient classification," in *Proc. Adv. Neural Inf. Process. Syst.*, 1999, pp. 678–684.
[23] G. Z. Karabulut, T. Kurt, and A. Yongacoglu, "Optical CDMA detection by basis selection," *J. Lightw. Technol.*, vol. 23, no. 11, pp. 3708–3715, Nov. 2005.
[24] C.-Y. Chang, C.-C. Wang, G.-C. Yang, M.-F. Lin, Y.-S. Liu, and W. C. Kwong, "Frequency-hopping CDMA wireless communication systems using prime codes," in *Proc. IEEE 63rd Veh. Technol. Conf.*, vol. 4, May 2006, pp. 1753–1757.
[25] W. C. Kwong and G.-C. Yang, *Optical Coding Theory With Prime*. Boca Raton, FL, USA: CRC Press, 2018.
[26] W. C. Kwong, W. Lin, G. Yang, and I. Glesk, "2-D optical-CDMA modulation in automotive time-of-flight LiDAR systems," in *Proc. 22nd Int. Conf. Transparent Opt. Netw. (ICTON)*, Jul. 2020, pp. 1–4.
[27] G. Kim, I. Ashraf, J. Eom, and Y. Park, "Concurrent firing light detection and ranging system for autonomous vehicles," *Remote Sens.*, vol. 13, no. 9, p. 1767, May 2021.
[28] F. Lo, G. Yang, W. Lin, I. Glesk, and W. C. Kwong, "2-D optical-CDMA modulation with hard-limiting for automotive time-of-flight LiDAR," *IEEE Photon. J.*, vol. 13, no. 6, pp. 1–11, Dec. 2021.
[29] G. Lee, J. K. Park, and J. T. Kim, "OCDMA codeword switching technique to avoid interference of time-of-flight LiDAR system for autonomous vehicles," *IEEE Sensors J.*, vol. 23, no. 3, pp. 3090–3102, Feb. 2023.
[30] W. C. Kwong and G.-C. Yang, "An algebraic approach to the unequal-spaced channel-allocation problem in WDM lightwave systems," *IEEE Trans. Commun.*, vol. 45, no. 3, pp. 352–359, Mar. 1997.
[31] J. D. McClure, "Diode laser radar: applications and technology," in *Proc. SPIE*, vol. 1219, pp. 446–456, May 1990, doi: 10.1117/12.18283.
[32] W. C. Kwong and G.-C. Yang, "Multiple-length multiple-wavelength optical orthogonal codes for optical CDMA systems supporting multirate multimedia services," *IEEE J. Sel. Areas Commun.*, vol. 22, no. 9, pp. 1640–1647, Nov. 2004.
[33] W. C. Kwong, G.-C. Yang, and Y.-C. Liu, "A new family of wavelength-time optical CDMA codes utilizing programmable arrayed waveguide gratings," *IEEE J. Sel. Areas Commun.*, vol. 23, no. 8, pp. 1564–1571, Aug. 2005.
[34] W. C. Kwong, G.-C. Yang, V. Baby, C.-S. Bres, and P. R. Prucnal, "Multiple-wavelength optical orthogonal codes under prime-sequence permutations for optical CDMA," *IEEE Trans. Commun.*, vol. 53, no. 1, pp. 117–123, Jan. 2005.
[35] C.-P. Hsieh, C.-Y. Chang, G.-C. Yang, and W. C. Kwong, "A bipolar-bipolar code for asynchronous wavelength-time optical CDMA," *IEEE Trans. Commun.*, vol. 54, no. 7, pp. 1190–1194, Jul. 2006.
[36] F. Zeng, Q. Wang, and J. Yao, "Sequence-inversion-keyed optical CDMA coding/decoding scheme using an electrooptic phase modulator and fiber Bragg grating arrays," *IEEE J. Sel. Topics Quantum Electron.*, vol. 13, no. 5, pp. 1508–1515, Oct. 2007.
[37] S. Murakami and A. Tsuneda, "A study on SIK optical CDMA communications using orthogonal binary sequences," in *Proc. 14th Int. Symp. Commun. Inf. Technol. (ISCIT)*, Sep. 2014, pp. 427–430.
[38] J. S. Lee and L. E. Miller, *CDMA Systems Engineering Handbook*. Norwood, MA, USA: Artech House, 1998.
[39] E. Ghillino, E. Virgillito, P. V. Mena, R. Scarmozzino, R. Stoffer, D. Richards, A. Ghiasi, A. Ferrari, M. Cantono, A. Carena, and V. Curri, "The synopsys software environment to design and simulate photonic integrated circuits: A case study for 400G transmission," in *Proc. 20th Int. Conf. Transparent Opt. Netw. (ICTON)*, Jul. 2018, pp. 1–4.
[40] G. Kim and Y. Park, "Independent biaxial scanning light detection and ranging system based on coded laser pulses without idle listening time," *Sensors*, vol. 18, no. 9, p. 2943, Sep. 2018.
[41] *VLS-128 User Manual*, Velodyne LiDAR, San Jose, CA, USA, 2018.
[42] Q. Abdullah, D. Maune, D. C. Smith, and H. K. Heidemann, "New standard for new era: Overview of the 2015 ASPRS positional accuracy standards for digital geospatial data," *Photogramm. Eng. Remote Sens.*, vol. 81, no. 3, pp. 173–176, 2015.
[43] American Society for Photogrammetry and Remote Sensing, "ASPRS positional accuracy standards for digital geospatial data," *Photogramm. Eng. Remote Sens.*, vol. 81, no. 3, pp. 1–26, 2015.

GUNZUNG KIM (Member, IEEE) was born in Daegu, Republic of Korea, in 1972. He received the B.S. and M.S. degrees in computer engineering and the Ph.D. degree in multimedia and communication engineering from Yeungnam University, Republic of Korea, in 1995, 1997, and 2019, respectively. He is currently a Research Professor with Yeungnam University. His research interests include LiDAR, optical communication, and vehicle software.

JEONGSOOK EOM was born in Daegu, Republic of Korea, in 1975. She received the B.S. and M.S. degrees in computer engineering from Yeungnam University, Republic of Korea, in 1998 and 2001, respectively, where she is currently pursuing the Ph.D. degree in multimedia and communication engineering. Her research interests include LiDAR, optical communication, and mutual interference between active sensors.

YONGWAN PARK (Member, IEEE) was born in Daegu, Republic of Korea, in 1959. He received the B.E. and M.E. degrees in electrical engineering from Kyungpook University, Daegu, in 1982 and 1984, respectively, and the M.S. and Ph.D. degrees in electrical engineering from The State University of New York at Buffalo, USA, in 1989 and 1992, respectively. He is currently a Professor with Yeungnam University and also the Chairperson of the 5G Forum Convergence Service Committee in Republic of Korea. His current research interests include 5G systems in communication, OFDM, PAPR reduction, indoor location-based services in wireless communication, and smart sensors (LiDAR) for smart cars.